

Supplementary Information for

Exosomes regulate Neurogenesis and Circuit Assembly

Pranav Sharma^{1,2*}, Pinar Mesci^{3,4*}, Cassiano Carromeu^{3,4}, Daniel McClatchy⁵, Lucio Schiapparelli^{1,2}, John R Yates III^{1,5}, Alysson R. Muotri^{3,4,6,7}, Hollis T Cline^{1,2†}

¹The Scripps Research Institute, Neuroscience Department, La Jolla, California 92093, USA

²The Scripps Research Institute, The Dorris Neuroscience Center, La Jolla, California 92093, USA

³University of California San Diego, School of Medicine, Department of Pediatrics/Rady Children's Hospital San Diego, La Jolla, California 92093, USA.

⁴University of California San Diego, School of Medicine, Department of Cellular & Molecular Medicine, La Jolla, California 92093, USA.

⁵The Scripps Research Institute, Department of Chemistry, La Jolla, California 92093, USA

⁶University of California San Diego, Kavli Institute for Brain and Mind, La Jolla, California 92093, USA.

⁷Center for Academic Research and Training in Anthropogeny (CARTA), La Jolla, California 92093, USA.

*co-first authors

† Lead Author, to whom correspondence should be addressed:
Dr. Hollis Cline, 10550 North Torrey Pines Rd. La Jolla, CA 92037.
cline@scripps.edu

This PDF includes
List of antibodies.
Figs S1 to S8
Legends for datasets S1-S11

Other supplementary materials for this manuscript include:

Dataset S1-S11

List of antibodies:

No	Antibody (host)	Supplier	Cat #	Dilution used
1	Anti-Synapsin I (rabbit)	Synaptic Systems	106 002	1:500 (IF*)
2	Anti-MAP2 (mouse)	Eurogentec	M1406	1:500 (IF*)
3	Anti-Nestin (mouse)	Eurogentec	MMS-570P	1:500 (IF*)
4	Anti-GFAP (rabbit)	DAKO	Z033429-2	1:1000 (IF*)
5	Anti-Doublecortin (mouse)	Abcam	ab135349	1:200 (IF*)
6	Anti-AIP1/Alix (rabbit)	Millipore	ABC40	1:1000 (WB**)
7	Anti-Flotilin (rabbit)	Sigma Aldrich	F1180	1:1000 (WB**)

*IF=Immunofluorescence, **WB=Western Blot

Supplemental Figure 1.

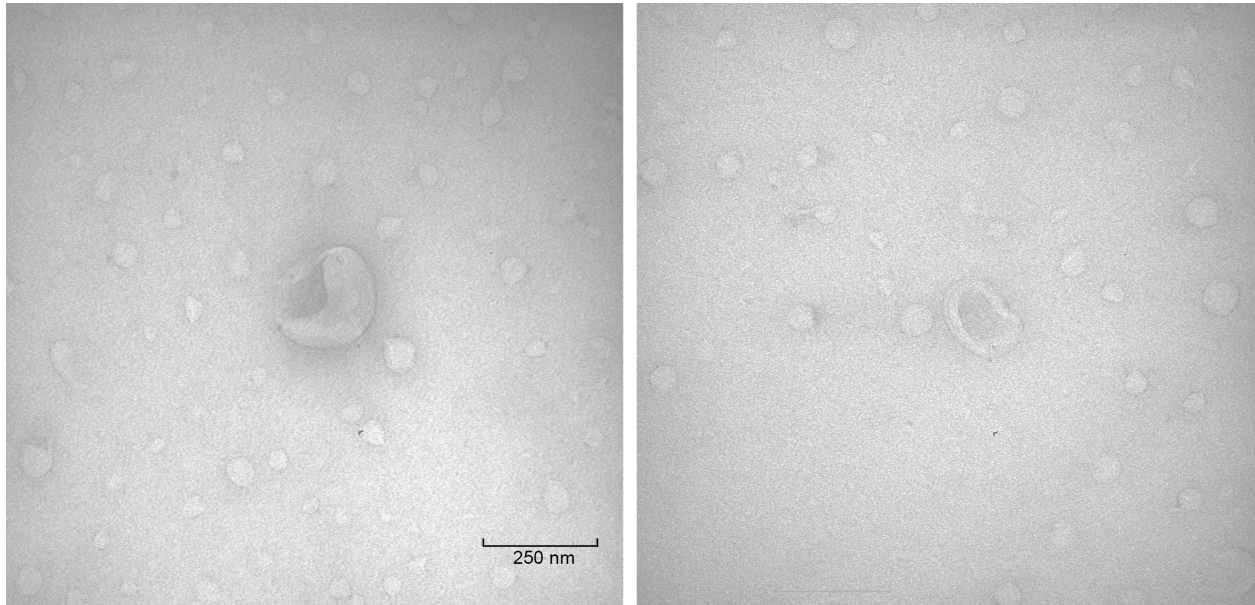


Fig S1. Electron micrographs of purified exosome preparations. Exosomes were enriched from serum-free media from hiPSC-derived neural cultures as described in Figure 1A. The harvested media was centrifuged at 300g for 15 minutes at 4°C, the supernatant was collected and centrifuged at 2000g for 15 minutes at 4°C in a Beckman tabletop centrifuge. The second supernatant was further centrifuged using a Beckman ultracentrifuge at 10,000g for 45 min at 4°C. The supernatant was collected and centrifuged at 100,000g for 1 hour at 4°C to pellet exosomes. We applied purified exosomes to a grid covered by carbon and negatively stained them with 1% uranyl acetate (Faure et al., 2006). EM analysis of negative staining of exosomes indicate that the sizes of these vesicles are compatible with those described for exosomes purified from other cells.

Supplemental Figure 2.

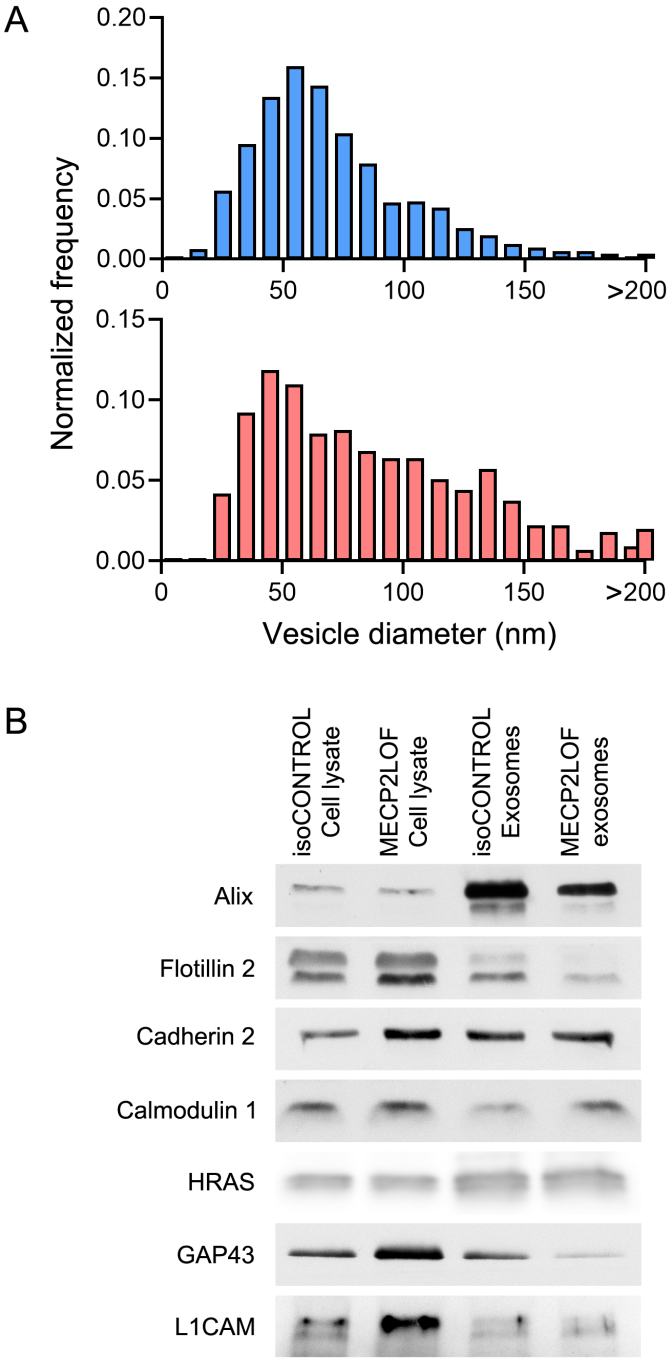


Fig S2. A, Size distribution of exosomes purified from human iPSC-derived control (top, blue) and MECP2LOF (bottom, red) neural cultures. Vesicle diameter was calculated from electron micrographs. B. Western blot analysis showing distribution of proteins in cells lysates vs exosomes from isoCONTROL and MECP2LOF iPSC-derived neural cultures.

Supplemental Figure 3.

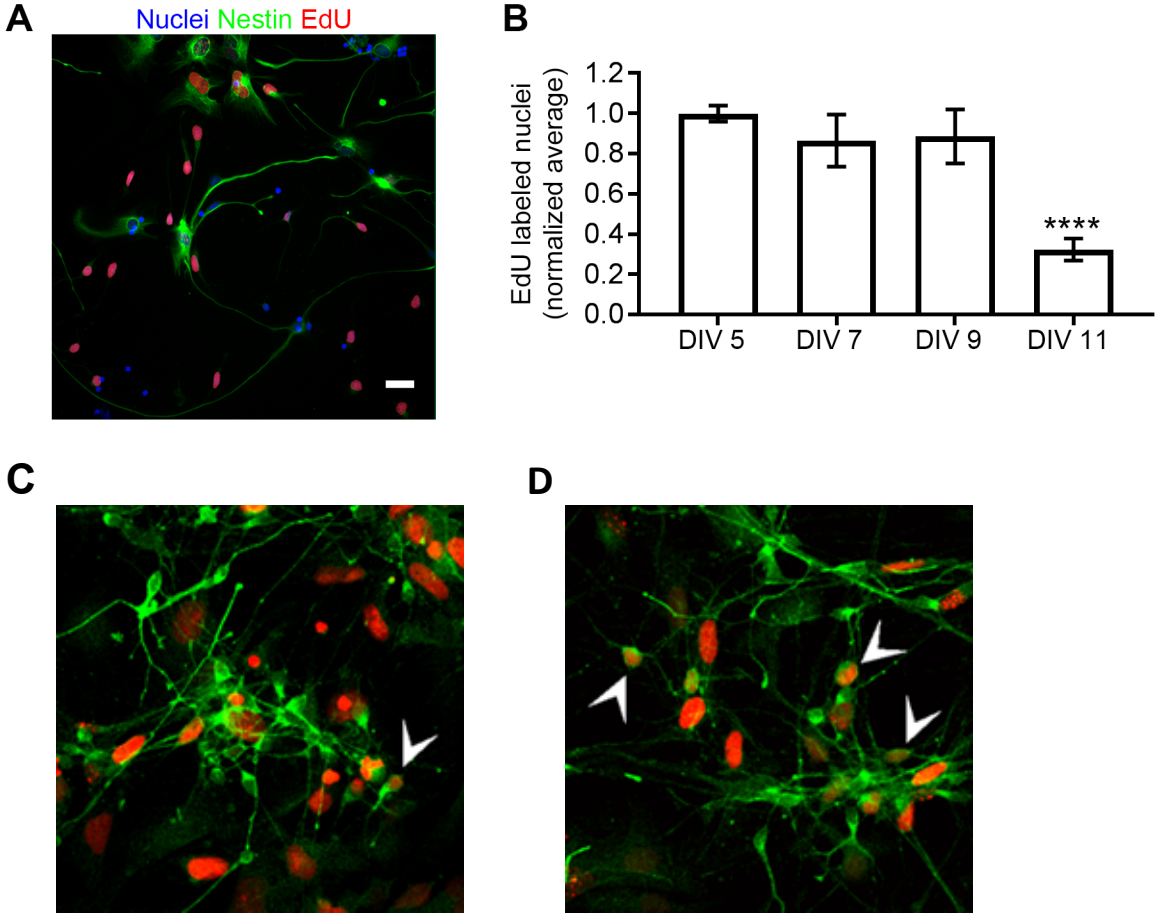


Fig S3. Primary human neural cultures include progenitor cells. Control exosome treatment increases neurogenesis. A. Image of human primary neural cultures immunolabelled with EdU (red) and Nestin (green), showing neural progenitor cells (NPCs) that co-label with EdU. B. To test whether human primary neural cultures maintain proliferative activity over 11 DIV, cultures were treated with EdU for 4 hours on DIV 5, 7, 9 and 11 and immediately fixed. Cultures were immunolabeled for EdU and counterstained with DAPI and analyzed to determine the number of EdU immunolabeled cells, normalized to DAPI+ nuclei. Data for each timepoint were then normalized to 5 DIV. EdU incorporation in human primary neural cultures was constant over 5-9 DIV and then dropped significantly to $32.3 \pm 5.5\%$ compared to DIV 5 ($p=0.0001$, two-way ANOVA with Bonferroni correction) at DIV 11. N= 4 wells each. C. 3X zoom from figure 3F. D. 3X zoom from figure 3G.

Supplemental Figure 4.

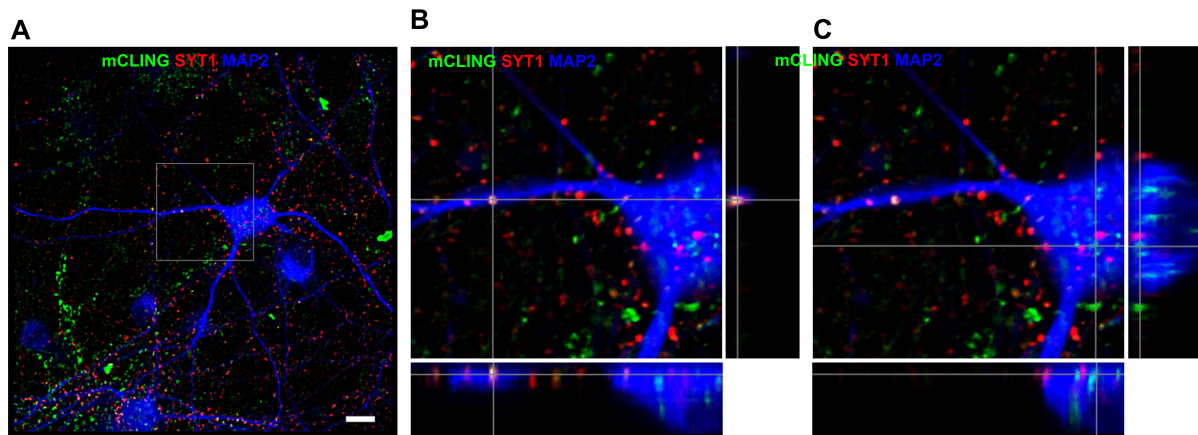


Fig S4. Exosome uptake into cultured neurons. To investigate whether exosomes are taken up by neurons, we labeled purified exosomes with fluorescent membrane label, ATTO 488 mCLING (Revelo et al., 2014). Labeled exosomes were added to hiPSC-derived neural cultures. After 4 hours, cultures were fixed and immunolabeled with the neuronal marker, MAP2, and the synaptic marker, synaptotagmin 1 (SYT1). A-C. Z-merged composite image from 3-D confocal microscopy analysis showed mCLING labeled exosomes inside MAP2-labeled neurons. The majority of mCLING label was present as punctate labeling around nucleus. B. Insets shown at 2.5X zoom with Y-Z plane (right) and X-Z plane (bottom) intersecting at synaptotagmin 1 (SYT1) labeled puncta show that mCLING label is present in SYT1 puncta along the neuronal processes. The puncta with mCLING and SYT1 labels are juxtaposed to a MAP2 labeled process. C. Insets shown at 2.5X zoom with Y-Z plane (right) and X-Z plane (bottom) intersecting at the cell body shows that mCLING label is present inside the cell body. These data indicate that exogenously added exosomes are taken up by neurons in neural cultures and distributed to different cellular compartments, including synapses.

Supplemental Figure 5.

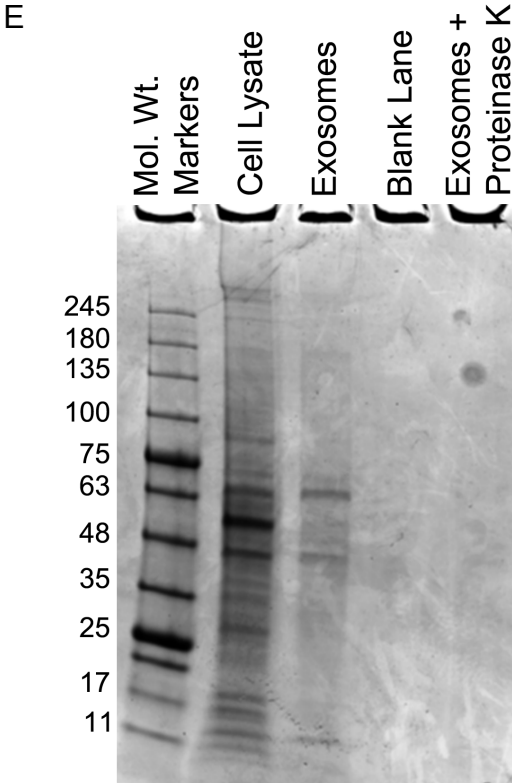
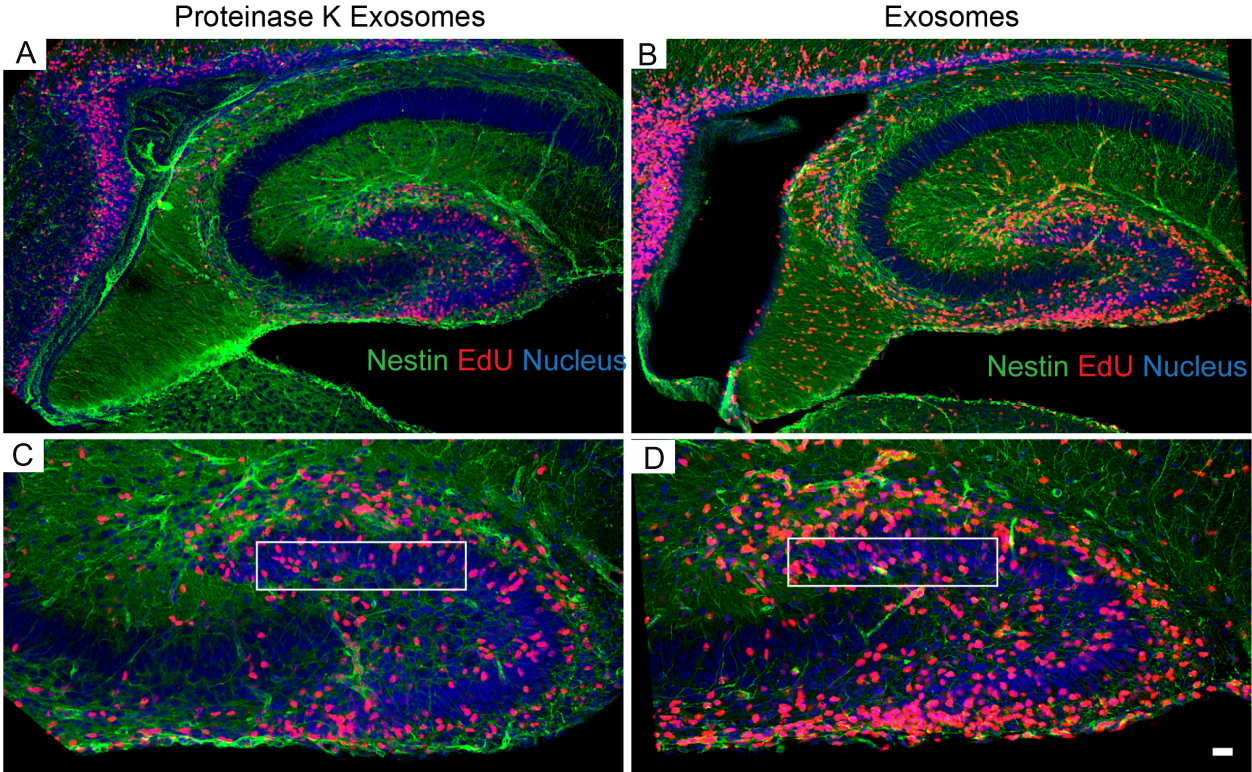
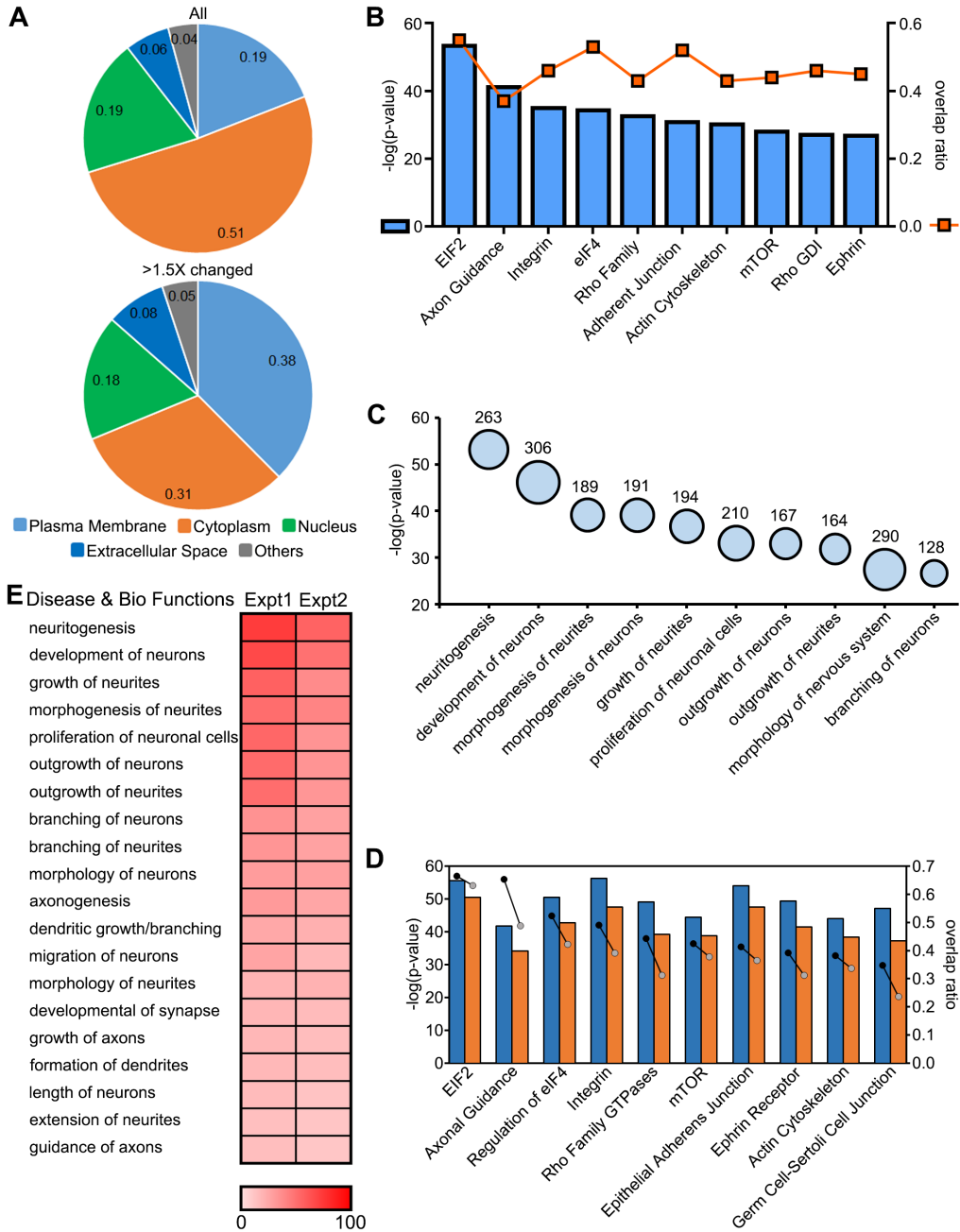


Fig S5. Sagittal sections through hippocampus to identify matched regions of dentate gyrus. Sagittal sections through mouse brains were labeled with EdU+ cells (red), Nestin (green) immunolabeling and TO-PRO-3 nuclear stain (blue), and anatomically matched sections were identified in brains from animals treated with exosomes. A,B. Low magnification images showing hippocampus and overlying cortex. C,D. Higher magnification images through hippocampus and dentate gyrus showing representative regions of interest used to quantify EdU+ cells. Scale bar = 20 μ m. E. Western blot of exosome preparations treated with Proteinase K or PBS, stained with Coomassie Blue shows that Proteinase K depletes exosomes of proteins.

Supplemental Figure 6



Supplemental Figure 6: Analysis of exosome proteomics. Comparison between experimental replicates and identification of complex signaling components that are altered with MeCP2 mutation. Two independent MS experiments were performed each with 3 different MECP2LOF preparations and 3 different control preparations obtained from at least 3 independent batches of neuronal differentiations of NPCs for each line. Together, 6 biological replicates were analyzed together in each MS experiment. We detected 3611 and 3019 annotated proteins in experiment 1 and 2, respectively, with 2572 proteins (62% overlap) detected in both MS experiments. Of these, 873 and 789 proteins in experiments 1 and 2, respectively, were annotated for function in neurons with 739 detected in both (80% overlap). We compared these datasets to identify 'cellular pathways' and 'downstream effects on biological functions in the nervous system' using the manually curated Ingenuity database (Calvano et al., 2005). The two experiments provided very similar prediction results regarding 'cellular pathways' with p -values and overlap ratios (the fraction of proteins annotated for each pathway that were detected in the experimental dataset) ranging from 10^{-56} to 10^{-21} for p -values and 0.65 to 0.44 for overlap ratios for the top 10 pathways. Similarly, analysis of 'downstream effects on biological function in nervous system' demonstrated excellent reproducibility between the two experiments with p -values ranging from 10^{-73} to 10^{-37} for the top 10 categories. The analysis performed on the 2572 proteins that were overlapping between the 2 experiments was largely similar to results from individual experiments. A. Pie charts showing the cellular distribution of proteins identified in quantitative proteomic analysis of exosomes isolated from isogenic control and MeCP2LOF iPSC-derived neural cultures based on annotation using Ingenuity. The dataset of 237 proteins with >1.5 fold difference between control and MeCP2LOF exosomes was enriched in plasma membrane proteins compared to the dataset of all 2572 exosome proteins. B. Top 10 canonical pathways from Ingenuity analysis using the combined dataset of all 2572 exosome proteins. Blue bars, plotted on the left Y axis show significance values as $-\log(p\text{-value})$ and the orange squares, plotted on the right Y axis, show the overlap ratios of the number of proteins from our dataset relative to total number of proteins annotated to each canonical pathway. C. Bubble chart showing Ingenuity analysis of the relative

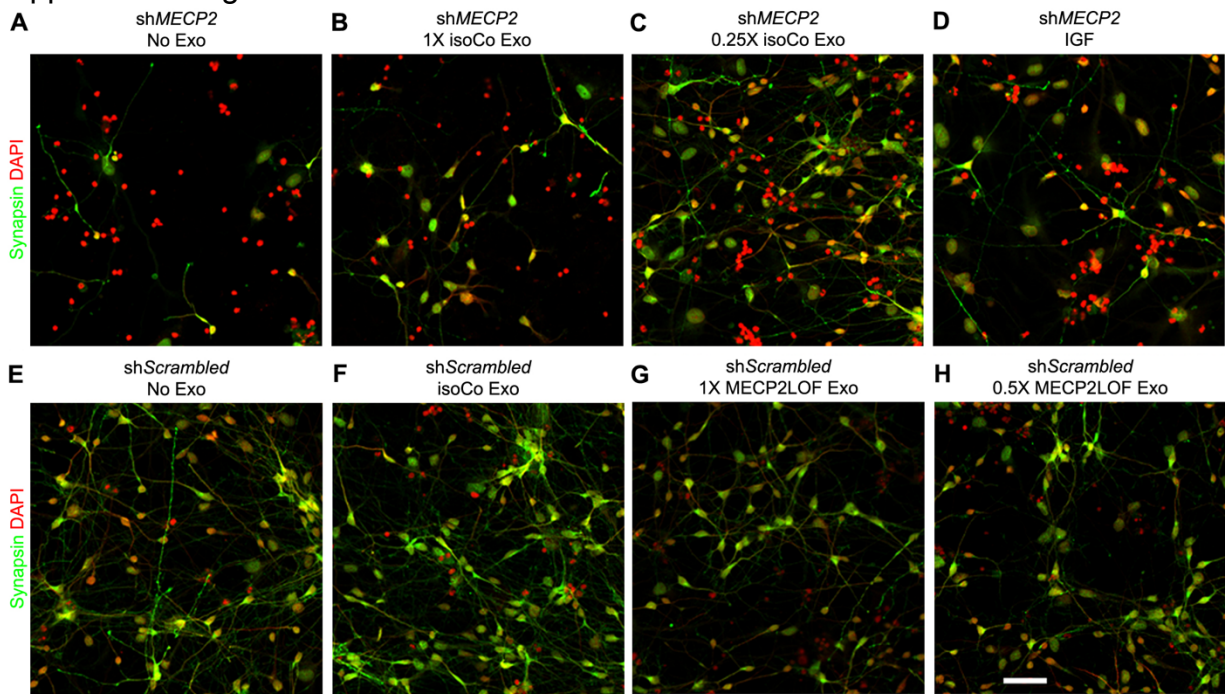
strength of downstream effects for biological functions and diseases in the nervous system using the dataset of all 2572 exosome proteins. The top 10 predicted biological functions are plotted vs significance values, as $-\log(p\text{-values})$, where the bubble size represents the number of proteins from the dataset annotated for the given function. The data values for bubble size are shown on top of the bubbles. D. Comparative analysis of the top 10 canonical pathways from Ingenuity analysis using the data from two experimental replicates, experiment 1 (blue bars, black circles) and 2 (orange bars, grey circles). Bars, plotted on the left Y axis, show significance values as $-\log(p\text{-value})$. On the right Y axis, the circles show overlap ratios of the number of proteins in our experimental dataset versus the total number of proteins annotated by IPA to each canonical pathway. E. Comparative Ingenuity analysis of the relative strength of the categories “downstream effects for biological functions” and “diseases in the nervous system” for the two experimental replicates, experiments 1 and 2. The significance values are plotted as $-\log(p\text{-value})$ heatmap ranging from 0, white to 100, red (represented by LUT at the bottom). Proteomic data are deposited at ExoCarta and Vesiclepedia.

Supplemental Figure 7

Synaptic vesicular neurotransmitter transporters
Vesicular glutamate transporter 1 (VGLUT1) Vesicular glutamate transporter 2 (VGLUT2) Vesicular glutamate transporter 3 (VGLUT3) Vesicular GABA transporter (VGAT, VIAAT) Vesicular acetylcholine transporter (VAChT) Vesicular Monoamine Transporter 1, 2 (VMAT)
Early endosomal marker
Early endosome antigen 1 (EEA1)
Endosome and plasma membrane markers
Caveolin 1 (CAV1) Caveolin 2 (CAV2) Nerve growth factor receptor (NGFR/p75)
Other markers
Lysine-specific demethylase 1 (LSD1) - Nucleus Lamin A/B/C - Nucleus Cytochrome C oxidase complex - Mitochondria

Supplemental Figure 7. List of markers absent from the exosome proteome.

Supplemental Figure 8



Supplemental Figure 8. Control exosomes rescue the reduced number of neurons and resulting from MeCP2 knockdown. A-D. Wide field fluorescence images show DAPI (red) and synapsin 1 (green) labeled cultures with MeCP2 scrambled shRNA knockdown treated with media (No Exo, A), 1X control exosomes (Co Exo, B), 0.25X control exosomes (0.25X Co Exo, C) and 10 ng/ml IGF (D) as described in Figure 5A. The images represent 3.5X zoom of images in Figure 4B, C bottom panel. E-H. Wide field fluorescence images of DAPI (red) and synapsin 1 (green) labeled cultures with scrambled shRNA control treated with media (No Exo, E), 1X control exosomes (1X Co Exo, F), 1X MeCP2LOF exosomes (G) and 0.5X MeCP2LOF exosomes (H) as described in Figure 4A. The images show 3.5X zoom of images in Figure 4D, E bottom panel. Scale bar = 20 μ m.

Supplemental Dataset Legends

Dataset S1: Experiment 1 of quantitative proteomic analysis of control vs MeCP2LOF exosomes. Related to figure 2. Proteome of quantitative TMT analysis between control and MeCP2LOF exosomes. 3611 proteins were identified in experiment 1. Average ratio of control/ MeCP2LOF (column H, I) was calculated from three ratios (column D, E, F) from 6 replicates in each experiment.

Dataset S2: Experiment 2 of quantitative proteomic analysis of control vs MeCP2LOF exosomes. Related to figure 2. Proteome of quantitative TMT analysis between control and MeCP2LOF exosomes. 3019 proteins were identified in experiment 2. Average ratio of control/ MeCP2LOF (column H, I) was calculated from three ratios (column D, E, F) from 6 replicates in each experiment.

Dataset S3: Annotation of quantitative control vs MeCP2LOF proteome for cellular location and protein type: All proteins. Related to Figure 2. Cellular location (column D) and protein type (column E) annotation using Ingenuity Pathway Analysis software for Proteomic dataset of 2572 proteins overlapping in experiments 1 and 2 that were changed between control and MeCP2LOF exosomes.

Dataset S4: Annotation of quantitative control vs MeCP2LOF proteome for cellular location and protein type: >1.5 fold changed. Related to Figure 2. Cellular location (column D) and protein type (column E) annotation using Ingenuity Pathway Analysis software for Proteomic dataset 237 proteins out of 2572 in dataset 3 that were changed >1.5 fold between control and MeCP2LOF exosomes.

Dataset S5: PANTHER Overrepresentation Test of proteins changed >1.5 fold between control and MeCP2LOF exosomes using the GO 'biological processes' complete annotation dataset. Related to Figure 2. PANTHER Overrepresentation Test of the dataset of 237 proteins with >1.5 fold change using the GO 'biological processes' complete annotation dataset. The 237 candidates were classified into annotated GO biological process categories (column A) and compared with the normal

human database (column B) to determine whether they are overrepresented or underrepresented (column E) and fold enrichment (column F) for a given GO biological process.

Dataset S6: Canonical pathways from Ingenuity Pathway Analysis of dataset of >1.5 fold changed proteins. Related to Figure 2. Canonical pathways from Ingenuity Pathway Analysis with -log p-value (column B) and overlap ratio (column C) for dataset of >1.5 fold differentially expressed proteins between control and MeCP2LOF exosomes. The proteins from dataset that are represented in pathway are listed in column D.

Dataset S7: Canonical pathways from Ingenuity Pathway Analysis of dataset of all proteins. Related to Supplemental Figure 6. Canonical pathways from Ingenuity Pathway Analysis with -log p-value (column B) and overlap ratio (column C) for dataset of all differentially expressed proteins between control and MeCP2LOF exosomes. The proteins from dataset that are represented in pathway are listed in column D.

Dataset S8: Relative strength of downstream effects for biological functions and diseases in the nervous system of dataset of >1.5 fold changed proteins. Related to Figure 2. Downstream effects for biological functions (column B and C) analysis by Ingenuity Pathway Analysis software in 'Nervous System Development and Function' category showing number of proteins from dataset (column D) and p-values (column E) for dataset of >1.5 fold differentially expressed proteins between control and Rett exosomes.

Dataset S9: Relative strength of downstream effects for biological functions and diseases in the nervous system of all proteins. Related to Supplemental Figure 6. Downstream effects for biological functions (column B and C) analysis by Ingenuity Pathway Analysis software in 'Nervous System Development and Function' category showing number of proteins from dataset (column D) and p-values (column E) for dataset of all differentially expressed proteins between control and Rett exosomes.

Dataset S10: Comparison analysis of Canonical Pathways between experimental replicates. Related to Supplemental Figure 6. Comparison analysis of canonical pathways using Ingenuity Pathway Analysis for experimental replicates, experiment 1 and 2 showing comparison of -log p-value (column C) and overlap ratio (column D) for each experimental replicate with proteins from dataset used for pathway listed in column E.

Dataset S11: Comparison analysis of downstream effect for biological functions between experimental replicates. Related to Supplemental Figure 6. Comparison of p-values (column B and C) between experimental replicates for downstream effects for biological functions analysis by Ingenuity Pathway Analysis software in 'Nervous System Development and Function' category.

Supplemental References

Calvano, S.E., Xiao, W., Richards, D.R., Felciano, R.M., Baker, H.V., Cho, R.J., Chen, R.O., Brownstein, B.H., Cobb, J.P., Tschoeke, S.K., *et al.* (2005). A network-based analysis of systemic inflammation in humans. *Nature* 437, 1032-1037.

Faure, J., Lachenal, G., Court, M., Hirrlinger, J., Chatellard-Causse, C., Blot, B., Grange, J., Schoehn, G., Goldberg, Y., Boyer, V., *et al.* (2006). Exosomes are released by cultured cortical neurones. *Mol Cell Neurosci* 31, 642-648.

Revelo, N.H., Kamin, D., Truckenbrodt, S., Wong, A.B., Reuter-Jessen, K., Reisinger, E., Moser, T., and Rizzoli, S.O. (2014). A new probe for super-resolution imaging of membranes elucidates trafficking pathways. *J Cell Biol* 205, 591-606.